SUBSURFACE DEFORMATIONS DETECTION IN SANDS UNDER TRAFFIC LOADS USING GROUND PENETRATING RADAR

Dr. Vijay Kumar Rayabharapu,
Associate Professor,
B V Raju Institute of Technology, Narsapur

ABSTRACT: Ground Penetrating Radar (GPR) is one of the most efficient non-destructive geophysical techniques used for subsurface investigations like detection of buried objects, underground life lines such as water mains, storage tanks and to some extent, void spaces in retaining structures and embankments. Identification of various shear failure surfaces generated due to static or cyclic loading on subgrade soils is very difficult. In this study, 1.6 GHz high frequency antenna has been used to predict the failure patterns of densified sand bed overlying weak subgrade layers in a $1m^3$ test tank, with and without geocell reinforcement. Radar-grams were generated before and after a repeated traffic load equivalent to the contact pressure of 550 kPa applied on the test bed. The radargrams obtained were analyzed using 3D Vision software for detecting the subsurface deformations.

Keywords: GPR, Traffic Loads, Deformations.

INTRODUCTION

An efficient pavement system should be free from any irregularities in pavement layers such as subsurface deflections and subsurface voids. The extent of these irregularities has to be determined in order to avoid the failure of the pavement system. To detect these irregularities, a number of destructive and non-destructive techniques are available.

As the name itself suggests, destructive tests like stress test, hardness test and crash tests can be done only by excavating or destructing the existing pavement layers, which in turn causes distress in the entire pavement system. The destructive testing methods cause disturbance to the traffic and it is time consuming.

Though several non-destructive testing methods like Falling weight Deflectometer (FWD) and Transient Dynamic Response (TDR) method are available, they have certain limitations like requirement of accurate layer thickness for data interpretation and expertise requirement respectively. Among the non-destructive testing methods, GPR is one of the most effective techniques used for various subsurface investigations.

The GPR applies a short pulse of electromagnetic energy (wave) into a material and records the amplitude and arrival time of reflected signals. When the pulse hits a material that has differentelectrical properties, a part of transmitted energy is reflected back and the remaining energy travels to the next interface. If a material is dielectrically homogeneous, then no major reflection will occur from within the layer. The amplitude of thereflection is determined by the contrast in the dielectric constants of the two materials. The dielectric constant defines the refractive index of the medium and also controls the speed of electromagnetic waves in the material [1].

The GPR equipment currently used for pavement characterization was developed over 25 years ago through two separate efforts: (1) the development of ground-coupled antenna systems for geological and geotechnical applications; and (2) the development of air-coupled horn antennas for mine detection. The ground-coupled equipment is optimal for deep penetration and where information is more qualitative rather than quantitative [2].

For a typical roadway survey with an air coupled GPR system, Eq. 1 governs the thickness-dielectric-density behavior. As shown in Fig. 1, the reflection A_1 is the energy reflected from the surface of the pavement; A_2 and A_3 are reflections from the top of the base and

subgrade layers respectively. These are all classified as positive reflections, which indicate an interface with a transition from a low to a higher dielectric material. These amplitudes of reflection and the time delays between reflections are used to calculate both layer dielectrics and thickness.

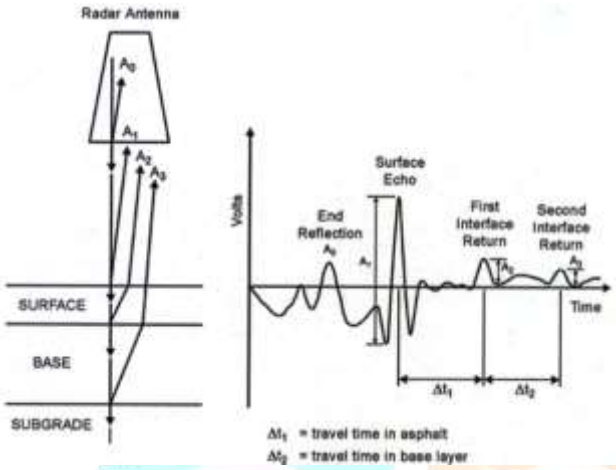

Fig. 1 Principle of GPR (Chen & Scullion-2007 [3])

$$\varepsilon_a = \left[\frac{1+\frac{A_1}{A_m}}{1-\frac{A_1}{A_m}}\right]^2 \quad (1)$$

Where, ε_a=the dielectric of the asphalt or concrete surfacing layer, A_1=the amplitude of reflection from the surface of the pavement in volts (peak A_1 in Fig. 1), and A_m=the amplitude of reflection from the aluminum metal plate in volts (this represents the 100 % reflection).

$$H_a = \frac{c.\Delta t_1}{\sqrt{\varepsilon_a}} (2)$$

Where, H_a=the thickness of the asphalt or concrete surfacing layer, c=a constant (speed of the radar wave in air as measured by the system), and Δt_1=the time delay between A_1 and A_2 of Fig. 1.

BACKGROUND

To check the pavement thickness, there was only coring or any excavation techniques available in the past. In the recent ten years, GPR has played a major role in determining the pavement thickness without any excavations or core samples.

According to Maser [2], GPR is an excellent tool for locating changes in the pavement structure and are clearly visible in the graphic display of the radar data. GPR can be used for pavement characterisation along with the pavement thickness measurement and also to determine the moisture within the asphalt pavement, which no other practical technique can measure.

Al-Qadi [4] stated that the basis for proposing radar (GPR) for moisture detection in, and under asphalt, is radar's strong sensitivity to moisture.

Hughes, et al. [5] stated that for quality control of new construction, GPR can provide the data equivalent to several hundred core samples.

Scullion and Saarenketo [6] showed that the merging of Falling Weight Deflectometer (FWD) data and GPR data was useful. The investigation was started with a high speed GPR survey to monitor the pavement thickness and to detect the defects in the pavement. Based on this survey, the FWD and the coring operations were done on the locations wherever necessary.

Chen and Scullion [7] and Uddin and Hudson [8] stated that in rehabilitation projects, GPR survey gives complete information about the existing profile and based on this information, the excavations were done to confirm the voids under the pavements and this in turn reduces the cost of coring or excavating the entire area and then construction of the same. In addition, Chen and Scullion [3] stated that the GPR was used to detect the air voids under major highways in Texas with reflections inverted of irregular patterns at the void location.

Leucci and Negri [9] showed the feasibility of GPR methodology in an urban area to locate the buried archaeological structures or monuments. The tests showed that with the help of a 3-D data, the idea of buried objects would be clearer.

According to Holt and Eckrose [10], GPR can be useful in various investigations like determination of voids and other utilities under the pavement, thickness of the pavement layer and the deteriorated regions of the pavement.

The main objective of this study is to detect the subsurface deflections caused due to the cyclic loading using GPR.

TEST SETUP

To identify the potential failure surfaces under a repeated load tests conducted in a model pavement system, a test tank with inner dimensions of 1m × 1m × 1m (length × width × height) was filled with sand of

30 % relative density up to a height H_1 to replicate weak subgrade and with 75 % relative density up to H_2 to replicate a dense base/sub base layer. The repeated traffic loading of intensity 550 kPa (equivalent to single axle wheel load exerted from a wheel base) was applied on to the bed through a rigid steel plate of 150mm diameter (D) and 15mm thickness. Based on the observations from Saride et al. [11] and Chummar et al. [12], the loading plate and the test tank dimensions were decided.

Similar kind of plate diameter and test tank was adopted by Edil et al. [13] in their laboratory experiments on geosynthetic reinforced pavements. The schematic representation of the test setup used in the present study is shown in Fig. 2. Loading was applied through a graphical user interfaced multi-purpose test software along with the help of a hydraulic power unit, hydraulic service manifold and sophisticated double acting linear dynamic 100kN capacity actuator which is connected to a 3.5m high, 200 kN capacity reaction frame as shown in Fig. 3.

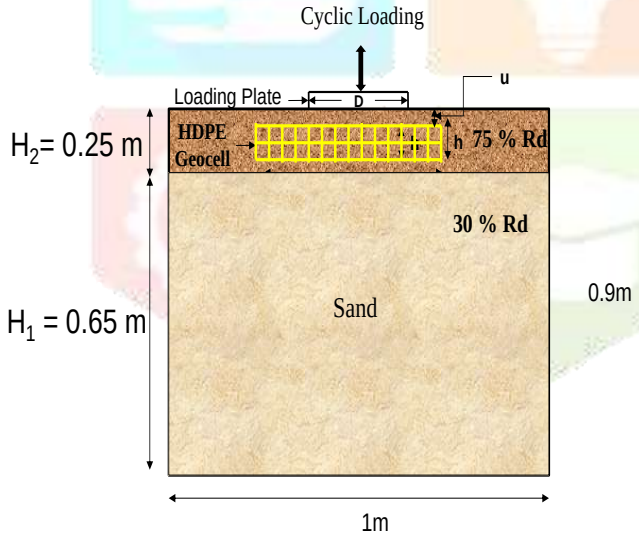

Fig. 2 Schematic representation of test setup

Fig. 3 Test tank and the loading system used in the study

TESTING PROCEDURE

After filling the test tank with sand, the surface was levelled and the loading plate was placed on the surface such that the loads from the actuator would be applied concentrically to the footing. In the case of reinforced beds, the sand was filled up to a desired depth and the geocell was positioned and stretched on the levelled subgrade and then the sand was pluviated to fill the geocell mattress with the same density. The repeated loads are applied by a computer controlled servo hydraulic actuator using a steel plate, with a load of 10kN which imparts a contact pressure of 550kPa. The loading pattern was chosen in such a way that it represents the live moving traffic on the pavement. The test generates a cyclic load – displacement relation for each test configuration adopted in the study. The repeated load tests are generally continued until they reach a failure condition. The failure in such tests can be defined as reaching a failure load corresponds to excessive settlements on the bed surface or reaching a prescribed settlement. In both the cases, the compacted soil below the loading area would undergo large deformations before it fails. Typically, one can expect a mode of general shear failure if the bed is

dense/stiff where the failure planes are expected to develop full and reach the ground surface. Weak foundation beds show either local or punching shear failure patterns. It is very necessary to identify these failure planes which will describe the behaviour of the pavement system.

A ground penetration radar (GPR) was used to identify such failure zones in the test bed before and after the repeated load is applied.

The GPR equipment used in this study was a 1.6 GHz high frequency antenna as shown in Fig. 4 and it is best suited for subsurface explorations like pavement characterisation upto a depth of about a meter.The antenna is capable of sending high frequency radar waves upto a meter depth and can be helpful in recording the images or radargrams of the same depth. The velocity of the shear wave passing through the uniformly densified sand was 0.120 m/ns. The GPR test was a 3-D grid project, which consists of traversingthe GPR antenna on the surface of the prepared sand bed along the length and across the width of the test tank in a grid pattern with a grid size of 0.1m × 0.1m and then tested with GPR.

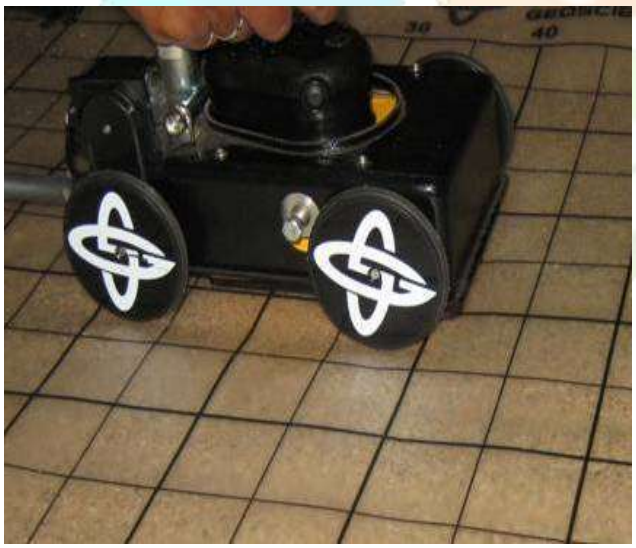

Fig. 4 1.6 GHz High Frequency GPR antenna

RESULTS AND DISCUSSIONS

The GPR surveys were performed on the test tank comprising of uniform relative density sand by dividing the entire tank area into a number of grids. The GPR antenna was run on the surface gridlines of the test tank before and after the application of the repeated loading for both unreinforced and geocell reinforced sand beds to generate a radar gram. Figure 5 shows the raw radargram generated through 1.6 GHz antenna.

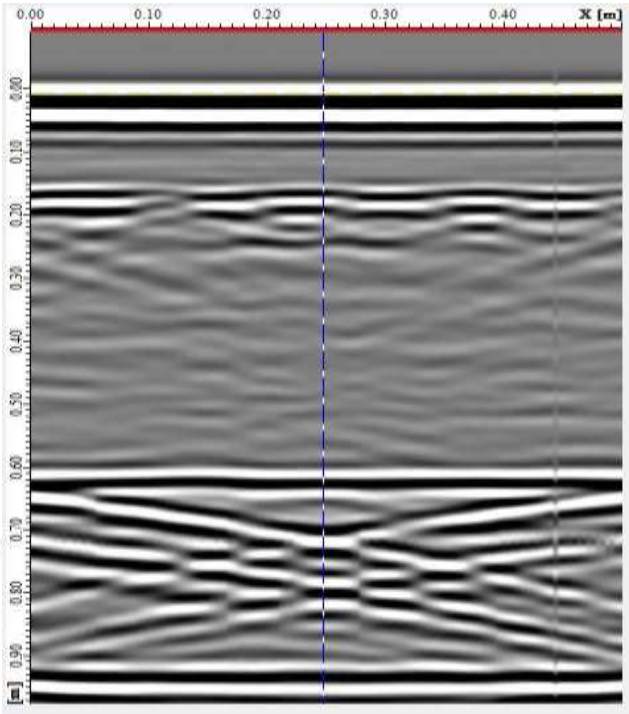

Fig. 5 Radargram before applying filters for unreinforced sand before cyclic loading test

After the radargram was generated, the raw data was analyzed by applying background removal filter, migration filter and fine tunings like sharpness and contrast. The background removal filter helps to minimize the air gap present between the bottom of the antenna and the surface of the test tank. The migration filter helps to remove the disturbance in the radargram due to obstructions while running the GPR on the surface of the test tank. It can be seen that dense reflections are recorded at the bottom of the test tank. At this location, the reflections are higher as the four sides and the bottom of the test tank are made up of iron. The excess application of filters to remove the metal tank reflections would also remove the failure patterns or shear planes generated due to cyclic loading. Fig. 6a shows the radargram after the application of filters and fine tuning as mentioned above.

The velocity of the shear wave passing through the different layers plays a major role. The velocity of shear wave has to be selected depending upon the type of the material and the dielectric constant of the material. Table 1 shows the different types of material and their corresponding dielectric constants and shear

wave velocities. It is to be noted that the decrease in the shear wave velocity decreases the depth of wave penetration into the layers below.

Table 1 Dielectrics and shear wave velocity [14]

Materials	Dielectric constant	Shear wave velocity (m/ns)
Air	1	0.300
Fresh water	81	0.033
Sand	4-30	0.055-0.150
Clay	4-16	0.074-0.150
Silt	9-23	0.063-0.100

In Figs. 6a, and 6b, the zone-A (top 0.2m) represents the uniformly densified sand layer with a relative density of 75%, the zone-B (below zone-A) represents the weak subgrade (sand) with a relative density of 30%. The zone-C in Fig. 6b represents the active stress concentration below the wheel loads (loading plate) after the application of cyclic loading. The reflections in the zone-D (0.6m -0.9m) are more prominent when compared with zones A-C because of the reverberation effect of the electromagnetic waves in the test tank with five sides made up of steel.

Figures 6a and 6b show radargrams of an unreinforced sand subgrade before and after the cyclic load application respectively. The black rectangular box at the top (at 0.0m) represents the tire load applied on the surface of the sand bed. A line at a depth of 0.2 m in both the Figures represents the location of pressure cells made of stainless steel which have highly reflected the electromagnetic waves generated from the antenna. Except these high intensity reflections at this location, the radargram shows fairly uniform plot. This represents the fairly well prepared test bed.

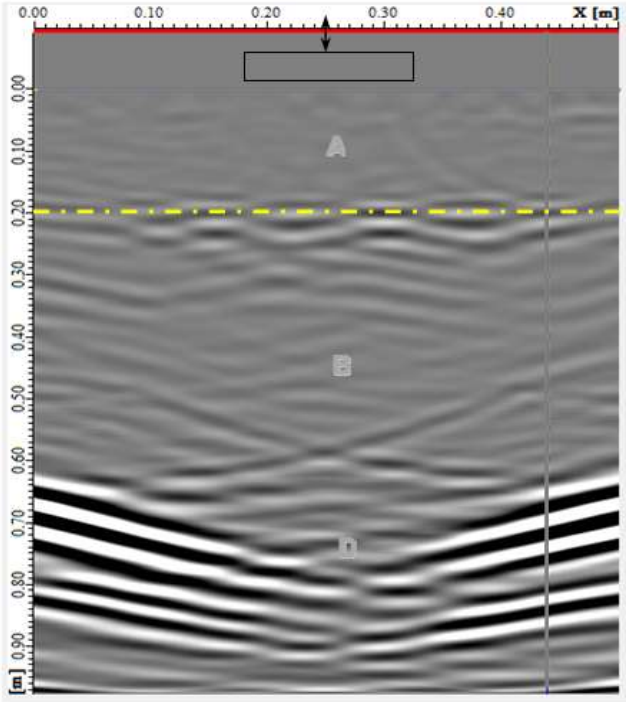

Fig. 6a Radargram of unreinforced sand bed before cyclic loading test

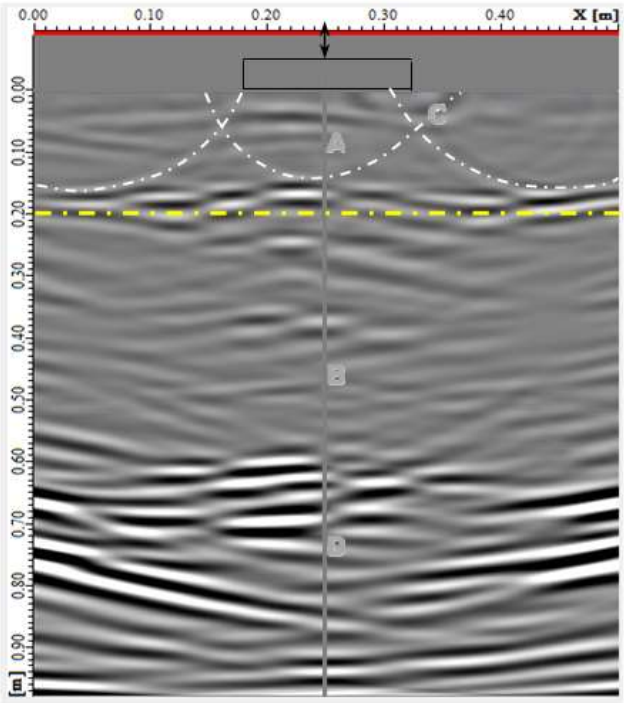

Fig. 6b Radargram of unreinforced sand bed after cyclic loading test

The white color dotted lines encountered in the radargrams from the test bed after the loading (Fig. 6b) represent potential shear failure planes generated in the sand bed which are predominantly appear above 0.2m. These shear planes resemble a general shear

failure, that can be expected in a dense sand with relative density of 75% in the present case. In this case, the failure took place at a very large strains. At failure, only a small portion of sand underneath the loading area participates and well defined rupture surfaces are developed exactly under the loading area. However, some disturbance can be seen in the lower weaker sand layers with 30% relative density (zone B). These shear planes depict that some compression has taken place in these layers at failure.

Similar radargrams were obtained from geocell reinforced dense sand beds overlying weak sand subgrades. The zones defined in Figs. 6a and 6b are also seen in Figs. 7a and 7b. In Fig. 7a, there are reflections also seen above line at 0.2m depth before the application of repeated loading because of the presence of extra earth pressure gauges placed within the geocell reinforcement. These reflections are not seen in Fig. 6a as there is no reinforcement or pressure gauges provided. The radargram in these cases also show reflections in the top 0.2m depth because of the change in density due to presence of geocell reinforcement.

From Fig. 7b, it can be inferred that there are no significant formation of continuous shear planes as the bed was reinforced with geocell, instead lateral confinement of sand layer was observed. It can be depicted that the shear planes are intermittent and observed in the geocell zone only.

However, after the application of cyclic loading, the radargrams for geocell reinforced sand bed varies significantly with that of unreinforced case. The presence of geocell as a reinforcement in the base layer helps to withstand the cyclic loading against failure or seizes the generation of the shear planes or deflections on the subsurface of the pavement.

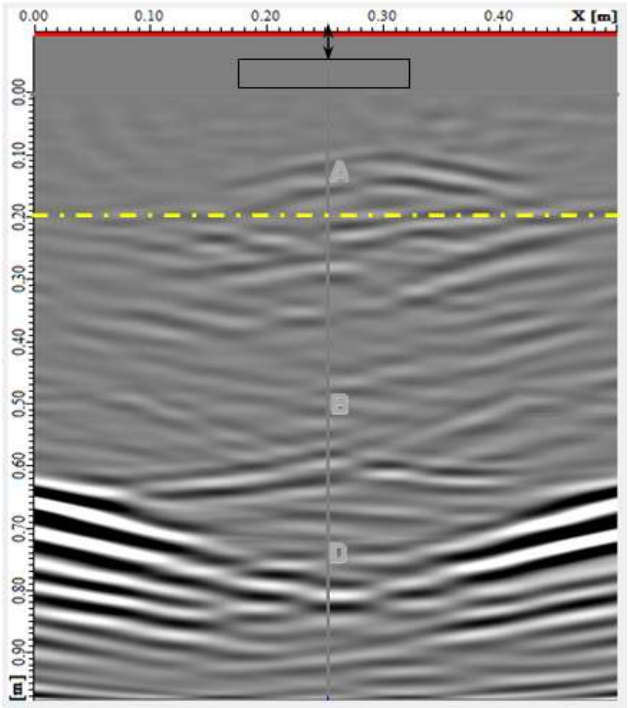

Fig. 7a Radargram of geocell reinforced sand bed before cyclic loading test

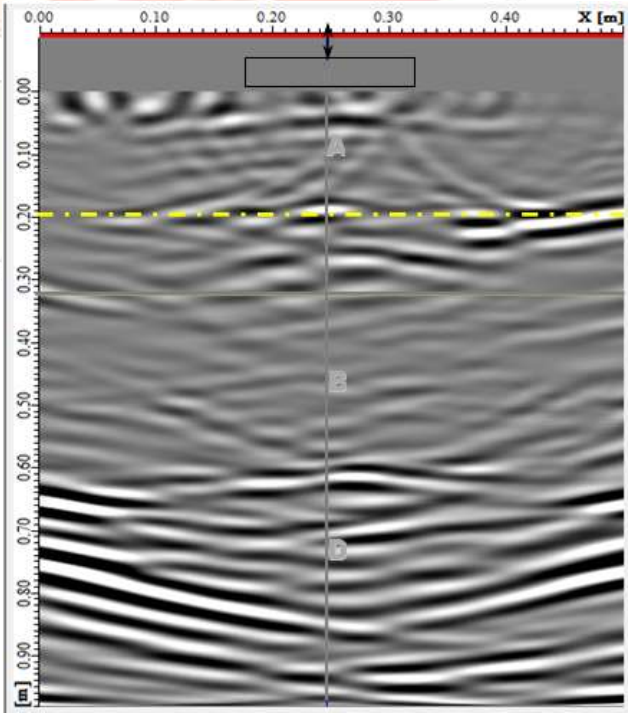

Fig. 7b Radargram of geocell reinforced sand bed after cyclic loading test

CONCLUSIONS

A series of non-destructive testing using ground penetration radar was carried out on dense sand beds over a weak sand subgrade with and without geocell reinforcement in the upper dense sand layers to identify the potential shear failure planes. Following are some of the major conclusions drawn from the study:

GPR is a non-destructive testing method that can be effectively utilized to predict the shear planes or the deflection patterns in a pavement layer.

GPR is a cost effective method for rehabilitation projects as the details of the entire pavement area is shown in the radargram, the defects can be directly corrected by means of coring or trenching.

The radargram from the unreinforced bed depicts that the dense sand layer undergoesa general shear mode of failure after the application of repeated loading.

The radargram also shows the presence of geosynthetic materials due to its high density. This observation infers that high quality radargrams can detect the geosynthetic material buried under pavements.

The presence of the shear planes or deflection patterns in case of the geocell reinforced sand beds is not prominent when compared to the unreinforced case.

REFERENCES

1. Cardimona, S., (2007), "*Subsurface Investigation Using Ground Penetration Radar*," http://www.dot.ca.gov/hq/esc/geotech/gg/geophysics2002/059cardimona_%20radar_overview.pdf.
2. Maser, K. R., (2000), "*Pavement Characterization Using Ground Penetrating Radar: State of the Art and Current Practice*," Non-destructive Testing of Pavements and Back calculation of Moduli: Third Volume, ASTM STP 1375.
3. Chen, D-H, and Scullion, T., (2007), "*Detecting Subsurface Voids Using Ground-coupled Penetrating Radar*," Geotech. Test. J., Vol. 31, No. 3.
4. AI-Qadi, I. L., (1990), "*Detection of Moisture in Asphaltic Concrete By Microwave Measurements*," Ph.D. Thesis, The Pennsylvania State University, College Park, PA.
5. Hughes, C. S., Simpson, A. L., Cominsky, R., Pendleton, O. J., Weed, R. M., and Wilson, T., (1996), "*Measurement and Specification of Construction Quality, Volume 1L Final Report*," FHWA Report DTFH61-94-C-O0078, Brent Rauhut Engineering Inc., Austin, TX 78759.
6. Scullion, T. and Saarenketo, T., (2000), "*Integrating Ground Penetrating Radar and Falling Weight Deflectometer Technologies in Pavement Evaluation*," Non-destructive Testing of Pavements and Back calculation of Moduli: Third Volume, ASTM STP 1375, S. D. Tayabji and E. O. Lukanen, Eds., American Society for Testing and Materials, West Conshohocken, PA.
7. Chen, D-H, and Scullion, T., (2006), "*Using Non-destructive Testing Technologies to Assist in Selecting the Optimal Pavement Rehabilitation Strategy*," J. Of Testing and Evaluation, Vol. 35, No. 2.
8. Uddin, W., and Hudson, R., (1994), "*Evaluation of NDT Equipment for Measuring Voids under Concrete Pavements*," Non-destructive Testing of Pavements and Back calculation of Moduli (Second Volume]. ASTM STP 1198, Harold L. Von Quintas, Albert J. Bush, III, and Gilbert Y. Baladi, Eds., American Society for Testing and Materials, Philadelphia.
9. Leucci, G., and Negri, S., (2006), "*Use of ground penetrating radar to map subsurface archaeological features in an urban area*," Journal of Archaeological Science, 33(4), pp502–512.
10. Holt, E. B., and Eckrose, R. A., (1989), "*Application of Ground-Penetrating Radar and Infrared Thermography to Pavement Evaluation*," Non-destructive Testing of Pavements and Back calculation of Moduli, ASTM STP 1026, A. J. Bush III and G. Y.

Baladi, Eds., American Society for Testing and Materials, Philadelphia, pp. 105-115.

11. Chummar, A. V., (1972), "*Bearing capacity theory from experimental results*," J GeotechEng ASCE 98(12):1311–1324.
12. Edil, T. B., Fratta, D., and Shuettpelz, C. C., (2009), "*Development of testing methods to determine interaction of geogrid-reinforced granular material for mechanistic pavement analysis*," Wisconsin DOT and FHWA Project Report.
13. Saride, S., Vijay, K. R., Suraj, V., (2014), "*Evaluation of Rutting Behaviour of Geocell Reinforced Sand Subgrades Under Repeated Loading*," Indian Geotech J.